World Conference on Timber Engineering Oslo 2023

AN EXPERIMENTAL STUDY ON SHEAR PERFORMANCE OF CLT DOWEL JOINTS WITH SHEAR PLATES

Tsuyoshi Akutagawa[1], Hiroya Hanaoka[2], Masamichi Sasatani[3],

ABSTRACT: Cross Laminated Timber (CLT) is often used in mid and high rise timber buildings, and there has been much research into its joints. In this paper, a dowel-type joint with a steel plate and shear plate between two CLTs are proposed, and experiments are carried out to gain knowledge of the shear capacity and stiffness of the joint. The variables in the experiment were the composition of a CLT, shear plate way of insertion, and end distances. The experimental results and Johansen's theory were used to study the stress transfer mechanism and to obtain equations for estimating the stiffness and shear capacity of the joints. The experimental results confirm the superiority of shear plates in terms of shear capacity and other factors.

KEYWORDS: Cross Laminated Timber, Shear plate, drift pins, Shear performance of dowel joint

1 INTRODUCTION

Due to global environmental issues, there is an active movement to develop timber architectures, and Cross Laminated Timber (CLT) is often used, especially in mid and high rise timber architectures. In this case, the performance of the building hinges on the performance of its joints, given the high rigidity of CLT panels. Various techniques are employed to enhance joint strength, including augmenting the diameter or quantity of connectors. In this study, our emphasis was on the use of shear plates as a means of enhancing the performance of single joints.

Shear plates are one type of joint employed in timber architectures, but not enough knowledge is available on combining them with CLT. A design of shear plate connections in CLT is beyond scope of NDS and AIJ [1-2].

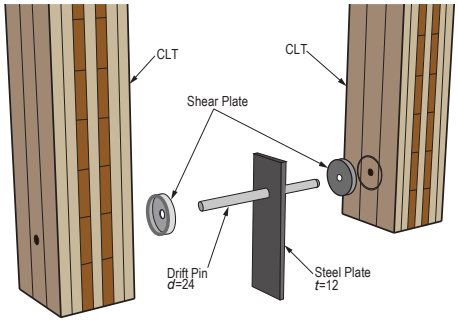

Figure1: *Image of the joint.*

In this study, we conducted experiments on joints that combined drift pins and shear plates, as shown in Fig. 1, and confirmed their shear capacity and stiffness properties. In addition, experimental results and Johansen's theory were used to estimate the load-bearing capacity using a simple equation.

2 TENSILE TESTING OF JOINTS

2.1 EXPERIMENT OVERVIEW

A list of specimens is in Table 1 and experimental variables are shown in Fig. 2.

Experimental variables were a composition of CLT (JAS standard grades: S90-5-7, S90-5-5, S60-3-4, and S60-3-3), way of insertion of shear plates, and end distance. The diameter of drift pins (d = 24 mm) and outer diameter of shear plates (D = 110 mm) used to join specimens were standardized for all variables. By CLT composition, four lengths were used, 417 mm, 297 mm, 237 mm, and 177 mm. Steel plates used for the joints were 12 mm thick, and holes for drift pins (φ=25 mm) were provided with a clearance of 1 mm. Between two CLTs, a plywood plate of a thickness equal to a steel plate was inserted.

A specimen is shown in Fig. 3.

Loading conditions were static monotonic loading and an application rate of 0.05 mm/sec. Displacement transducers were used to measure relative vertical displacement between each CLTs and steel plate at four locations, and mean values were used to evaluate results. An experiment was terminated when a load was reduced to 80% of a maximum load (Pmax) or when a displacement exceeded 25 mm.

[1] suyoshi Akutagawa, Graduate School of Tokyo Denki Univ., M.Eng., Japan, 21uda01@ms.dendai.ac.jp
[2] Hiroya Hanaoka, Graduate School of Tokyo Denki Univ., Japan, 22fma28@ms.dendai.ac.jp
[3] Masamichi Sasatani, Prof., Tokyo Denki University, Dr. Eng., Japan, sasatani@maill.dendai.ac.jp

https://doi.org/10.52202/069179-0188

Table 1: *Experimental variables*

Specimen name	Grade ※1	Composition	Insertion Type	End distance (mm)	Number carried out
J1-(i)-168	S90 5-7	7layer (t=210mm) Cypress	(i)	168	3
J1-(iii)-168			(iii)		3
J2-(i)-168	S90 5-5	5layer (t=150mm) Cypress	(i)	168	6
J2-(ii)-168			(ii)		6
J2-(iii)-168			(iii)		6
J2-(i)-240			(i)	240	6
J3-(i)-168	S60 3-4	4layer (t=120mm) Cedar	(i)	168	3
J3-(iii)-168			(iii)		3
J4-(i)-168	S60 3-3	3layer (t=90mm) Cedar	(i)	168	3
J4-(iii)-168			(iii)		3

※1 Conforms to the standards to the JAS (Japanese Agricultural Standards)

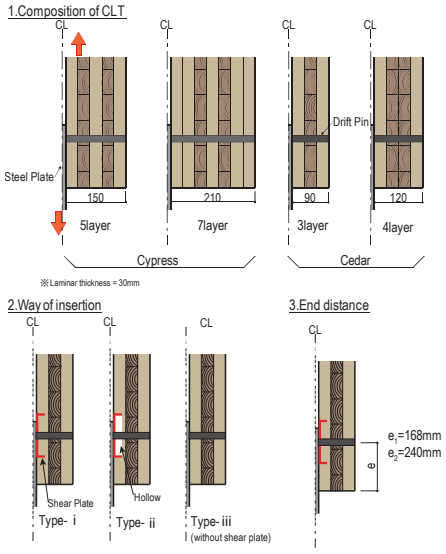

Figure2: *Experimental variables.*

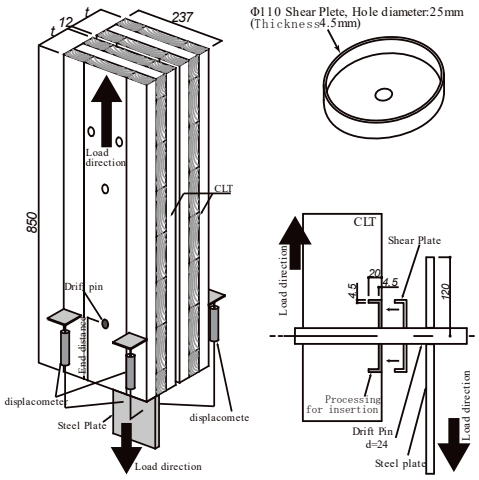

Figure3: *Shape of the test piece and test method.*

2.2 CATEGORIES OF FAILURE

The typical failure modes of CLTs identified at the end of experiments are shown in Fig. 5, the typical drift pin deformation states are shown in Fig. 6, and the categories of failure modes for all variables are shown in Table 2.
In both variables, out-of-plane deformation occurred in the two CLTs due to bending deformation of the drift pins because the CLTs were not constrained to open in the out-of-plane direction.
Four failure modes were observed at the end of experiments when specimens were disassembled as follows.
Mode [a]: embedded drift pin deformation only.
Mode [b]: Shear failure at the end of CLTs.
Mode [c]: Tensile failure of the orthotropic layers and shear failure to laminate surfaces.
Mode[d]: Tensile fracture near a finger joint of laminae on steel plate side.

A Comparison of the failure status of each variable confirms that the insertion of shear plates suppresses the deformation of a drift pin and that the thinner the CLT, the more likely it is to fail in the orthogonal layers.
Mode [a] failure was observed only in the Type-(iii) specimens. Failure of mode [b] was observed in Type-(i) and (ii) but not in Type-(iii). Modes [c] and [d] were observed at J3 and J4, possibly due to the thin CLT thickness, which resulted in large out-of-plane deformations. In particular, mode [d] could be attributed to the stress concentration at the bottom of the shear plate when the CLT was deformed out-of-plane and to the smaller edge distance due to the insertion of a shear plate.

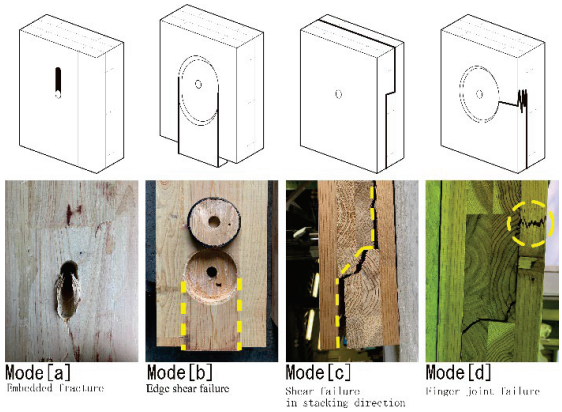

Figure5: *Final failure modes of CLTs.*

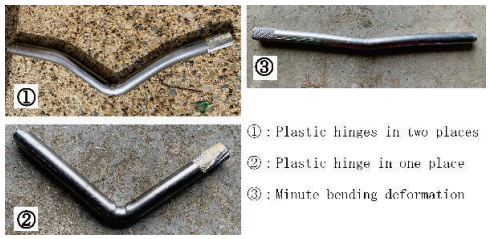

Figure6: *drift pin deformations.*

https://doi.org/10.52202/069179-0188

Table 2: *failures of all specimens.*

Specimen	No.					
	(1)	(2)	(3)	(4)	(5)	(6)
J1-(i)-168	b ③	b ③	b ③			
J1-(iii)-168	b ①	b ①	b ①			
J2-(i)-168	b ③	b ③	b ③	b + c ③	b ③	b ③
J2-(ii)-168	b ③	b ③	b ③	b ③	b ③	b ③
J2-(iii)-168	a ②	a ②	a ②	a ②	b ②	b ②
J2-(i)-240	b ③	b ③	b ③	b ③	b ③	b ③
J3-(i)-168	b +d ③	b + d ③	b + d ③			
J3-(iii)-168	b + c ②	c ②	b + c ②			
J4-(i)-168	b ③	b ③	b + c ③			
J4-(iii)-168	a ②	a ②	b + c ②			

2.3 EVALUATION OF JOINT TESTS

A typical load(P)-displacement(δ) curve is shown in Fig. 7, a yield load evaluation method is shown in Fig. 8, bearing capacity and stiffness for each variable are shown in Table 3, and a comparison of experimental results is shown in Fig. 9.

All variables showed initial slip (δ=1mm) for a clearance with a steel plate. After that, stiffness began to decrease when displacement was about 3 mm. Type-(iii) specimens showed increased displacement at a nearly constant load without significantly decreasing load. Type-(i) and Type-(ii) specimens continued to increase in load at about 50-60% of their initial stiffness after the stiffness drop was observed, and the load dropped abruptly at maximum load.

Table 3: *Results of tensile test of joints*

Specimen	Pmax [kN]		K[kN/mm]		Py ①		Py ②	
	mean	C.V. [%]	mean	C.V. [%]	mean	C.V. [%]	mean	C.V. [%]
J1-(i)-168	186.0	9.8	50.66	11.9	119.0	28.4	153.4	12.0
J1-(iii)-168	135.0	3.7	43.05	14.6	97.2	13.4	112.8	5.0
J2-(i)-168	178.0	6.7	53.04	23.6	93.0	11.5	155.5	9.5
J2-(ii)-168	187.6	8.1	54.8	10.9	108.1	19.3	172.2	7.8
J2-(iii)-168	145.2	4.9	59.1	44.8	103.0	10.8	112.5	11.1
J2-(i)-240	213.5	6.7	64.7	14.9	113.7	13.9	183.3	9.4
J3-(i)-168	141.0	9.9	30.42	5.4	97.6	8.2	129.2	1.8
J3-(iii)-168	95.9	9.2	35.51	17.5	71.1	7.1	78.3	8.8
J4-(i)-168	141.7	8.1	39.61	9.6	75.3	21.1	125.0	12.0
J4-(iii)-168	108.5	10.3	40.20	15.8	75.5	12.9	93.6	9.2

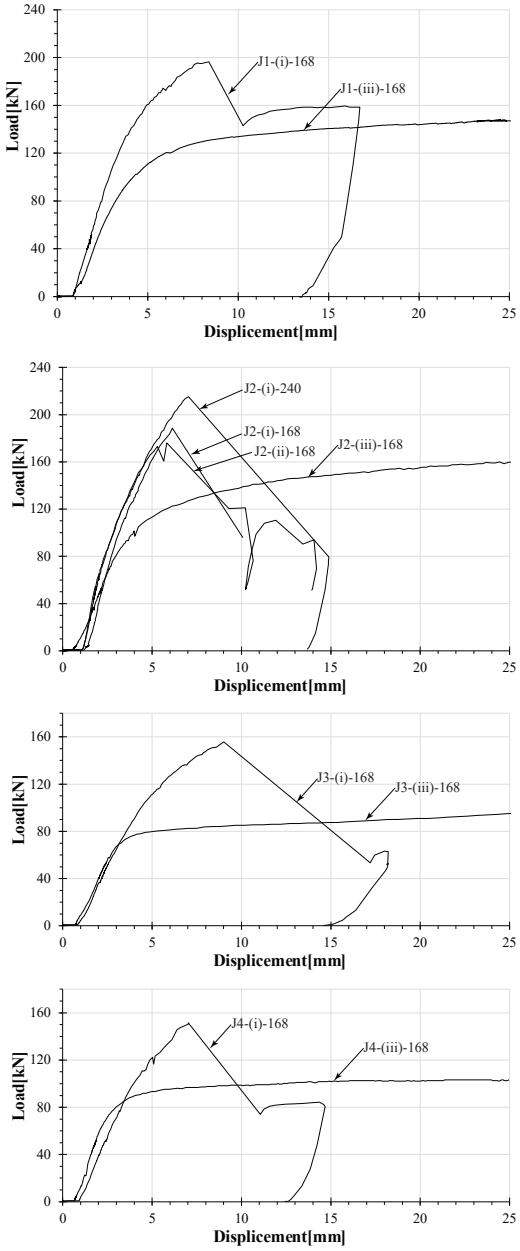

Figure7: *Relations between load and displacement*

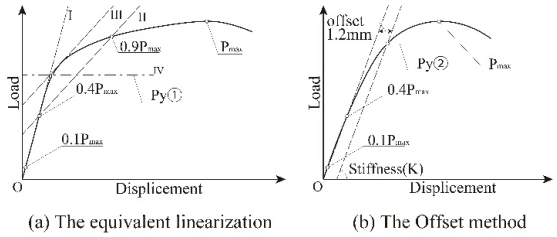

(a) The equivalent linearization (b) The Offset method

Figure8: *Yield load evaluation method*

Obtained stiffness and strength values are compared. For the maximum load, specimens of Type-(i) and (ii) were increased by 20-50% when compared to Type-(i). There

https://doi.org/10.52202/069179-0188

was no apparent difference in bearing capacity between Type-(i) and (ii), suggesting that the contribution of lumber inside a shear plate to the maximum load is small. No apparent increase or decrease in the stiffness was observed with a way insertion of a shear plate. It was considered that the clearance of holes for shear plate joints meant that a shear plate did not contribute to the stiffness. Yield loads differed significantly depending on the evaluation method. When the offset method(Py②) was used for evaluation, a 25-40% increase was observed for Type-(i) versus Type-(iii), and a 20% increase was observed for e=240mm versus e=168mm for the edge clearance distance e=240mm. On the other hand, when the equivalent linearization method[1] (Py①) was used for evaluation, the increase in bearing capacity was not as significant as the offset method. Depending on the variables, Type-(iii) showed higher results than Type-(i).

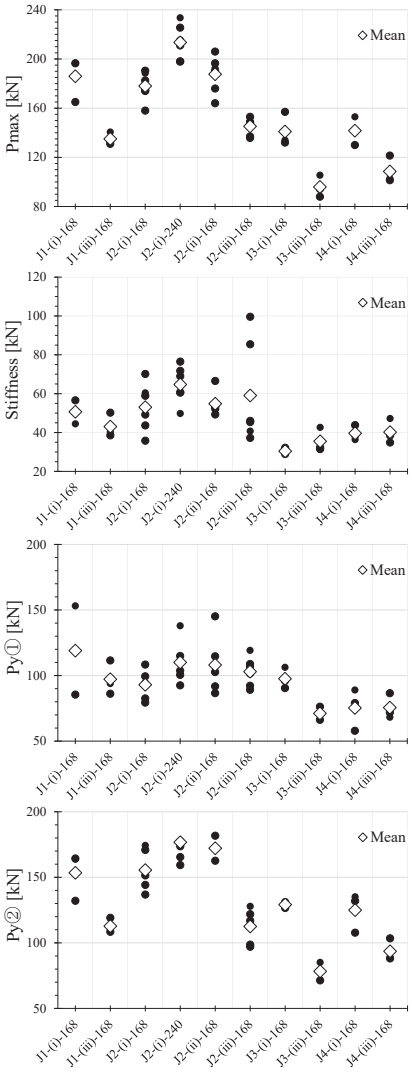

Figure9: *comparison of various property values.*

3 ESTIMATION OF LOAD CARRYING CAPACITY

3.1 EMBEDDING STRENGTH

Before estimating a joint's bearing capacity, an experiment was conducted to confirm CLTs' embedding strength (Fe). Experimental variables are shown in Table 4 and experimental results and specimen densities are shown in Table 5.

This study employed mean values of embedding strength to estimate yield capacities.

CLTs used in experiments were cut from the same panels as those used in Chapter 2, and four variables (S90-5-7, S90-5-5, S60-3-4, and S60-3-3) were conducted. The Dowel diameter (d) used for force application was 24 mm, and embedding strength was checked using the offset method (offset value was 1.2 mm) [3].

In this study, mean values of embedding strength were employed to estimate yield capacities.

Table 4: *Experimental variables (embedding test)*

Specimen	Grade	Composition	Thicness t [mm]	Specimen size
A-1	S90	5-7 (Cypress)	210	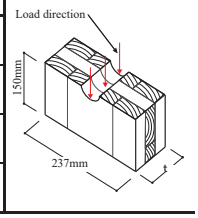
A-2		5-5 (Cypress)	150	
A-3	S60	3-4 (Cedar)	120	
A-4		3-3 (Cedar)	90	

Table 5: *Results of embedding test*

Specimen	Number Carried out	Density Mean [g/cm^3]	Embedding Stress [N/mm^2]
A-1	6	0.476	34.68
A-2	6	0.485	30.04
A-3	6	0.438	22.17
A-4	6	0.36	18.27

3.2 CALCULATION MODEL

Although previous studies have proposed evaluation formulas that consider the ratio of bearing strength for each lamina [4-6], in this study, the yield load was evaluated using equation (1) to simplify the formulas.

$$P_y = C \cdot d \cdot l \cdot F_e \quad (1)$$

Where *Py*: yield strength (kN), *C*: coefficient of joints type, *d*: pin diameter (mm), *l*: effective length of drift pin (mm), and *Fe*: embedding strength of lumber (N/mm2).

C in equation (1) assumes the case of a joint with a steel plate inserted. The equations for calculating *C* in 3 failure modes shown in Fig. 10 are below. The following minimum values are used in equation (1).

https://doi.org/10.52202/069179-0188

$$Mode1: C = 1.0 \tag{2}$$

$$Mode2: C = \sqrt{2 + \frac{8}{3}\gamma\left(\frac{d}{l}\right)^2} - 1 \tag{3}$$

$$Mode3: C = \frac{d}{l}\sqrt{\frac{8}{3}\gamma} \tag{4}$$

Where γ: ratio of material strength (F) of the drift pin to the reference bearing strength of the main material (F/Fe).

For joints with shear plates, *C* is similarly calculated for three failure modes. An assumed stress state is shown in Figure 10. In this case, the stress transmitted through a shear plate ($Fe \cdot D$) is not considered because this stress has a smaller shear span ratio than other stresses. The following equations express formulas for the forces and moments applied to the drift pins in each mode.

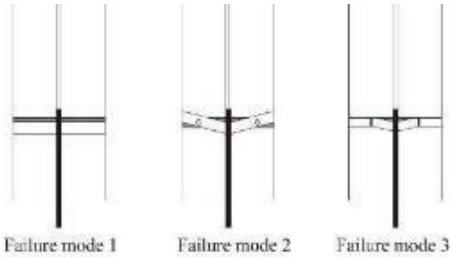

Figure10: *Failure modes.*

$Mode1$

$$\frac{P_y}{2} - F_e \cdot D \cdot h - F_e \cdot d \cdot \frac{l}{2} = 0 \tag{5}$$

$Mode2$:

$$\begin{cases} \dfrac{P_y}{2} - F_e \cdot D \cdot h - F_e \cdot d \cdot (x-h) + F_e \cdot d \cdot \left(\dfrac{l}{2} - x\right) = 0 \\ M_y - F_e \cdot d \cdot \dfrac{(x^2 - h^2)}{2} + F_e \cdot d \cdot \dfrac{\left(\left(\frac{l}{2}\right)^2 - x^2\right)}{2} = 0 \end{cases} \tag{6}$$

$Mode3$:

$$\begin{cases} \dfrac{P_y}{2} - F_e \cdot D \cdot h - F_e \cdot d \cdot (x-h) + F_e \cdot d \cdot \left(\dfrac{l}{2} - x\right) = 0 \\ M_y - F_e \cdot d \cdot \dfrac{(x^2 - h^2)}{2} + F_e \cdot d \cdot \dfrac{\left(\left(\frac{l}{2}\right)^2 - x^2\right)}{2} = 0 \end{cases} \tag{7}$$

Solving each simultaneous equation yields *C* for a joint with a shear plate, expressed by the following equation.

$Mode1$:

$$C = 1 - \alpha + \alpha\beta \tag{8}$$

$Mode2$:

$$C = \sqrt{2(\alpha^2 + 1) + \frac{8}{3}\gamma\left(\frac{d}{l}\right)^2} - 1 - \alpha + \alpha\beta \tag{9}$$

$Mode3$:

$$C = \sqrt{\alpha^2 + \frac{8}{3}\gamma\left(\frac{d}{l}\right)^2} - \alpha + \alpha\beta \tag{10}$$

Where *D* = outer diameter of shear plates (mm), h = depth of shear plate (mm), *My* = plastic moment of drift pin ($F \cdot d^3/6$ (N/mm)), α = ($2h/l$), β = (D/d), *x* = variable representing drift pin rotation center or plastic hinge position (mm).

For the embedded strength (Fe) in Equations (1), (2) through (4) and (8) through (10), the diameter of drift pins and shear plates were not distinguished, and the results in Section 3.1 were used to examine the applicability of a yield load. The calculation model for Type-(ii) was performed without distinction within this study since no difference in bearing capacity due to different ways of insertion was experimentally observed.

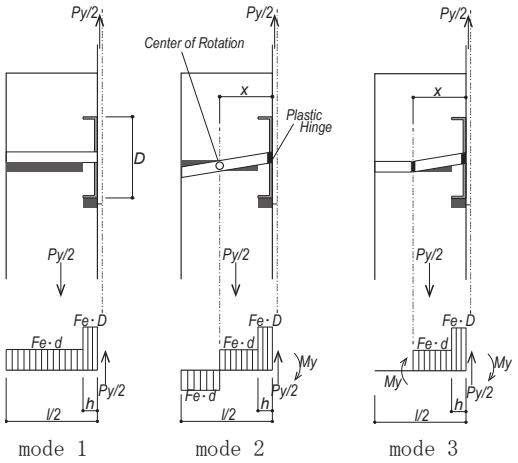

Figure11: *stress condition of joints with shear plates.*

3.3 ESTIMATED FAILURE MODE AND LOAD CAPACITY

Results of the calculation of *C* and estimated failure modes for each variable are shown in Table 6, and a comparison of calculation values and two experimentally obtained yield loads (Py① and Py②) is shown in Table 7. Colorized areas in Table 6 are the minimum values of *C*.

https://doi.org/10.52202/069179-0188

The deformation state of drift pins was generally similar to failure modes assumed from the calculated *C*. On the other hand, specimens Type-(i) and (ii) showed a sudden drop in load due to shear failure at the edge of CLT. A detailed study including shear failure is considered necessary in the following study.

Comparing two experimentally obtained yield loads with calculated values, evaluations using an equivalent linear replacement method tended to be slightly lower than calculated. Conversely, using the offset method, evaluation tends to be larger than calculated values. In addition to the fact that the embedding strength of each lamina was not considered to simplify this calculation, it is necessary to further examine experimental evaluation methods to improve calculation accuracy.

Table 6: *Calculation result for C*

Specimen	*d* [mm]	*l* [mm]	*h* [mm]	*D* [mm]	*F* [N/mm²]	F_e [N/mm²]	*C* mode1	mode 2	mode 3
J1-(i)-168	24	405	18	110	300	34.68	1.32	0.40	0.62
J1-(iii)-168	24	405	-	-			1.00	0.44	0.28
J2-(i)-168 J2-(ii)-168 J2-(i)-240	24	285	18	110	300	30.04	1.45	0.60	0.91
J2-(iii)-168	24	285	-	-			1.00	0.48	0.43
J3-(i)-168	24	225	18	110	300	22.17	1.57	0.83	1.23
J3-(iii)-168	24	225	-	-			1.00	0.55	0.64
J4-(i)-168	24	165	18	110	300	18.27	1.72	1.12	1.62
J4-(iii)-168	24	165	-	-			1.00	0.71	0.96

Table 7: *Comparison of calculation results*

Specimen	$_{(cal)}Py$ [kN]	$_{(mean)}Py$① [kN]	$_{(mean)}Py$② [kN]	$_{(mean)}Py$①/$_{(cal)}Py$	$_{(mean)}Py$②/$_{(cal)}Py$
J1-(i)-168	138.88	119.05	153.45	0.86	1.10
J1-(iii)-168	98.78	97.22	112.76	0.98	1.14
J2-(i)-168	128.36	93.00	155.51	0.72	1.21
J2-(ii)-168	128.36	113.74	183.30	0.89	1.43
J2-(iii)-168	128.36	108.09	172.17	0.84	1.34
J2-(i)-240	93.05	102.98	112.51	1.11	1.21
J3-(i)-168	104.23	97.62	129.17	0.94	1.24
J3-(iii)-168	69.68	71.12	78.33	1.02	1.12
J4-(i)-168	87.18	75.33	124.96	0.86	1.43
J4-(iii)-168	55.16	75.55	93.57	1.37	1.70

4 CONCLUSIONS

The following conclusions can be drawn from this study.

(1) Four types of wood fracture properties and three types of drift pin deformation states were identified. Shear failure at the CLT edge is more pronounced when shear plates are used.
(2) The deformation state of the drift pins indicates that yielding is dominated by the drift pins and the penetration stress.
(3) The use of shear plates is expected to increase the maximum load by 20-50%. On the other hand, the contribution to stiffness was not so great.
(4) The calculation of the joint type of coefficient C used in the proposed equation showed that the failure conditions of the drift pins in the experiment and the assumed yielding mode were in general agreement.

In the future, more detailed studies will be required, such as evaluation methods of the experiments and consideration of the embedded strength of each lamina that constitutes the CLT.

REFERENCES

[1] AIJ:Standard for Structural Design of Timber Strucures, 2018

[2] National Design Specification for Wood Construction, American Forest & Paper Association ANSI/AF & PA、pp.120、2018.

[3] K. Sawata, M. Yasumura ： Determination of embedding strength of wood for dowel-type fasteners 、*Journal of Wood Science*, Vol.48, pp138-146, 2002.

[4] T.Uibel, H.J.Blaß:Load Carrying Capacity of Joints with Dowel Type fasteners in Solid Wood Panels, CIB-W18/39-7-5, 2006

[5] S. Nakashima, A. Kitamori, K. Komatsu: Evaluation of tensile performance of drift pinned joints with steel plate on cross laminated timber (in Japanese). *Journal of Structural and Construction Engineering*, 78(687):969-975, 2013.

[6] S. Nakashima, N. Miki, N. Akiyama, Y. Araki: Estimation of initial stiffness, yield load, and ultimate load for the clt drift pinned connection with steel inserted plate and experimental verification (in Japanese). *Journal of Structural and Construction Engineering*, 86(783):793-803,2021

[7] R. Tomitaka, M. Toda: Application of European Yield Theory to Laminated Timber composed of Lumber with any Thickness and Bearing Strength (in Japanese). *Summaries of Technical Papers of Annual Meeting, Architectural Institute of Japan*, Structures III, pp.555-556, 2018

[8] N. Suzuki, Y.Yamazaki, H.Sakata, N.Toba, Y.Nonaka: A study on yield strength of CLT connection using LSB and shear-ring (in Japanese). *Summaries of Technical Papers of Annual Meeting, Architectural Institute of Japan*, Structures III, pp.549-550, 2012

https://doi.org/10.52202/069179-0188